Journal of Tropical Biodiversity and Biotechnology
Volume 11, Issue 02 (2026): jtbb24767
DOI: 10.22146/jtbb.24767

Research Article

Morpho-anatomical Characterisation and DNA Barcode of *Physalis angulata* L.

Samsurizal M. Suleman[1]*, Manap Trianto[1], Aan Febriawan[1], Bahana Aditya Adnan[2]
1)Departement of Biology Education, Faculty of Teacher Training and Education, Tadulako University. Jl. Soekarno Hatta No.99, Tondo, Palu Tim., Palu, Central Sulawesi 94111, Indonesia
2)Departement of Biology Education, Faculty of Teacher Training and Education, Galuh University. Jl. R.E. Martadinata No. 150, Ciamis, Mekarjaya, Baregbeg, Kec. Baregbeg, Jawa Barat 46274, Indonesia
* Corresponding author, email: biosamriz@gmail.com

Keywords:
Anatomy
DNA Barcoding
matK
Morphology
Physalis angulata
Phylogeny
Submitted:
21 September 2025
Accepted:
26 November 2025
Published:
18 May 2026
Editors:
Ardaning Nuriliani
Liya Audinah

ABSTRACT

Physalis angulata L. is a medicinally important species traditionally used to treat fever, inflammation, and metabolic disorders, making its accurate identification essential for safe pharmaceutical use. This study aims to identify *P. angulata* through an integrated morpho-anatomical approach and DNA barcoding. A total of 30 individuals from three populations in Central Sulawesi (Parigi Moutong, Sigi, and Donggala) were sampled for morphological characterization, while three representative individuals were used for anatomical analysis and matK sequencing. Morphological traits were assessed for leaves, stems, flowers, and fruits; anatomical features were examined through transverse and paradermal sections using the paraffin method; and DNA barcoding targeted the chloroplast *matK* region (~700–750 bp). The *matK* gene was successfully amplified and sequenced for all samples (n = 3), showing 100 % identity and full query coverage with *P. angulata* accessions in GenBank, and phylogenetic reconstruction clustered all sequences within a single well-supported clade. Morphological data revealed intraspecific variation in leaf and fruit characters, whereas stem and floral traits remained stable across populations. Anatomical observations showed a single-layered epidermis with sinuous cell walls, anomocytic stomata, and collateral vascular bundles with included phloem. Together, these findings provide robust integrative evidence confirming the identity of *P. angulata* and establish baseline morpho-anatomical and molecular data that can support future pharmacognostic, taxonomic, and conservation research.

How to cite:
Suleman, S.M. et al., 2026. Morpho-anatomical Characterisation and DNA Barcode of *Physalis angulata* L.. *Journal of Tropical Biodiversity and Biotechnology*, 11(2), jtbb24767. doi: 10.22146/jtbb.24767

INTRODUCTION

Physalis angulata L. commonly known as cutleaf groundcherry or "ciplukan" in Indonesian, an herbaceous plant belonging to the family Solanaceae. This species is widely distributed in tropical and subtropical regions and is well known for its medicinal properties (Firdaus et al. 2022; Prasetyawan et al. 2024). Traditionally, *P. angulata* has been used as a remedy for various ailments, including fever, inflammation, diabetes, and liver disorders (Mirzaee et al. 2019; Rivera et al. 2019; Novitasari et al. 2024). Its bioactive compounds, such as physalins, withanolides, and flavonoids, have been reported to possess significant pharmacological activities, including anti-inflammatory, antimicrobial, antioxidant, and anticancer properties (Ahmed et. al. 2023). Given its high medicinal value, *P. angulata* has attracted increasing scientific attention, not only for phytochemical and pharmacological investigations but also for its potential as a sustainable resource for herbal medicine development (Dini et al. 2022; Elhawary et al. 2025).

Despite its importance, research on the morphological and anatomical characterisation of *P. angulata* remains limited (Azeez et al. 2024). Morphological and anatomical studies play a crucial role in plant taxonomy because they provide fundamental information for the identification, classification, and differentiation of plant species (Rouhan & Gaudeul 2020). These studies are particularly important for medicinal plants, where accurate identification is necessary to ensure the quality, safety, and efficacy of herbal medicines. Misidentification or adulteration of medicinal plant materials can lead to reduced therapeutic effects or even harmful consequences (Yue et al. 2021; Malik et al. 2022; Wang et al. 2024). Therefore, detailed morpho-anatomical descriptions of *P. angulata* are essential for developing identification keys and supporting pharmacognostic standardisation (Kumar et al. 2022).

In addition to morphological and anatomical data, molecular tools have become increasingly important in plant identification and systematics. DNA barcoding, which uses short standardised regions of DNA as molecular markers, has emerged as a reliable approach for species identification (Ahmed et al. 2022; Antil et al. 2023). Among several DNA regions proposed for plant barcoding, the maturase K (*matK*) gene located in the chloroplast genome is widely used due to its relatively high rate of nucleotide substitution, which provides sufficient variation for distinguishing closely related species (Ebigwai et al. 2020; Leelavathy & Sankar 2021). The *matK* gene has been recommended as a core barcode region for land plants. Its high discriminatory power, coupled with universal primer availability, makes *matK* an effective marker for molecular identification and phylogenetic studies (Corvalán et al. 2025).

Combining morpho-anatomical characterisation with DNA barcoding provides a comprehensive approach to plant identification (Wahyuni et al. 2022, 2024). Morphological traits are easily observable but may be influenced by environmental factors, developmental stages, and phenotypic plasticity (Schneider & Meyer 2017). Anatomical characteristics, on the other hand, are relatively stable and less affected by external conditions, providing additional diagnostic value (Bolboacă 2019). Meanwhile, molecular markers such as *matK* offer precise and objective identification at the genetic level (Corvalán et al. 2025). An integrative approach that combines these methods not only improves the accuracy of plant identification but also contributes to building reference data for biodiversity documentation and conservation efforts (Wahyuni et al. 2024). This study aims to (1) describe morpho-anatomical variation among populations, and (2) test whether matK can unambiguously identify local specimens.

MATERIALS AND METHODS

Materials

The plant samples were collected in January 2025 from three regencies in Central Sulawesi Province, namely Parigi Moutong (PMR) (0°56'20"S 120° 14'08"E), Sigi (SR) (1°09'36"S 119°57'05"E), and Donggala (DR) (0°53'05"S 119°40'07"E). All specimens were obtained from secondary forest habitats and were collected by Samsurizal M Suleman and Manap Trianto.

The materials used in this study included *P. angulata* samples, FAA fixative solution (formalin, glacial acetic acid, and 70 % ethanol), graded alcohol series (50, 70, 95 %, and absolute), xylol, paraffin medium, safranin and fast green stains, Tiangen Plant Genomic DNA extraction kit, specific primers for the *matK* gene (Forward: 5' TGGTTCAGGCTCTTCGCTATTG 3' and Reverse: 5' CTGATAAATCGGCCCAAATCGC 3') (Do et al. 2019), GoTaq® Green Master Mix, 1 % agarose, 0.5X TBE buffer solution, and nuclease-free water.

The tools used in this study included a microtome, water bath, hotplate, incubator, glass slides and cover slips, a light microscope with 200–400× magnification, Thermo Scientific Multiskan Go, PCR thermocycler, UV transilluminator, and software such as BioEdit 7.4, BLAST online tool, and MEGA X.

Methods

Morphological Character Observation

The plant samples used for morphological characterisation were collected from three regencies in Central Sulawesi Province: Parigi Moutong (PMR), Sigi (SR), and Donggala (DR). In each regency, observations were conducted on 10 individual plants, resulting in a total of 30 sampled individuals. Morphological assessments were performed directly in the field, and measurements for each plant character (leaf, stem, flower, and fruit) were carried out with three replicates per plant part. The morphological characters examined included plant habit, leaves, stems, flowers, and fruits. Parameters for plant habit assessment included plant height, crown shape, and branching type. Stem characteristics included stem diameter and surface texture. Flower parameters followed Hasanuddin and Fitriana (2014), including flower position, symmetry, diameter, pedicel length, attachment type, and the number, length, and width of sepals and petals, as well as the number of stamens and the length of filaments and stigmas. Fruit characterisation referred to Susetyarini et al. (2020), consisting of fruit stalk length, calyx length and width, calyx vein colour, fruit length, and fruit diameter. All linear measurements were obtained using a digital caliper (Mitutoyo Absolute Digimatic Caliper 500-196-30; precision 0.01 mm, accuracy ± 0.02 mm).

Preparation of Microscopic Slides for Anatomical Structure Analysis

Anatomical structure analysis was conducted using two types of microscopic preparations, namely transverse and paradermal sections. Three *P. angulata* plants were used as samples. From each plant, three samples of leaves, stems, and roots were collected. The leaves used were the fourth leaves from different branches. The transverse section was prepared using the paraffin method. Samples were fixed in FAA solution, dehydrated using Johansen's alcohol series I–VII, infiltrated with paraffin, and embedded in paraffin blocks. The blocks were softened in Gifford solution, trimmed, mounted on a holder, and sectioned using a rotary microtome at a thickness of 15 µm. The paraffin ribbons were mounted on glass slides coated with glycerin-albumin adhesive. The sections were then stained with 2 % safranin and 0.5 % fast green. The stained preparations were mounted with entellan and covered with cover slips (Purnobasuki et al. 2017).

Paradermal sections were prepared from fresh leaf blades. The leaf surface was gently scraped with a toothpick on one side, then immersed in Clorox solution for 3 minutes and rinsed with distilled water. The sections were stained with safranin, mounted on glass slides with 30 % glycerin as the mounting medium, and covered with cover slips. The characters observed from the transverse leaf sections included epidermal thickness, palisade and spongy mesophyll thickness, leaf thickness, palisade ratio, and spongy mesophyll ratio.

The characters observed in the transverse sections of stems and roots include the number of layers and the shape of epidermal cells, the shape of cortical cells, the type, shape, and number of collenchyma cell layers, as well as the type of vascular bundle. The characters observed in the paradermal sections of leaves include the shape, size, and number of epidermal cells, as well as the type, index, and density of stomata. Observations of epidermal cell morphology, stomatal type, stomatal size, and stomatal density were conducted under a light microscope (Olympus CX23) at 200–400× magnification, and measurements were obtained using ImageJ calibrated to the microscope scale bar (Khan et al. 2017; Bello et al. 2017).

DNA Barcoding

DNA Extraction

The DNA extraction material consisted of young *P. angulata* leaves taken from the shoots. A total of three samples were used, each finely chopped into small pieces with a total weight of 0.1 g. DNA was isolated using the Tiangen Plant Genomic DNA Kit following the manufacturer's protocol. The concentration and purity of the extracted DNA were measured using a Thermo Scientific Multiskan Go.

Amplification and Sequencing

PCR amplifications were performed using GoTaq® Green Master Mix. Because a 2× master mix was used, each 35 µL PCR reaction contained 17.5 µL of 2× GoTaq® Green Master Mix (Promega), 1.75 µL of forward primer (10 µM; final concentration 0.50 µM), 1.75 µL of reverse primer (10 µM; final concentration 0.50 µM), 1.0 µL of genomic DNA template (approximately 50 ng; final template amount ~50 ng), and nuclease-free water to a final volume of 35.0 µL. The matK primers (Forward: 5'-TGGTTCAGGCTCTTCGC TATTG-3' and Reverse: 5'-CTGATAAATCGGCCCAAATCGC-3') were adopted from Do et al. (2019) and were used at a final concentration of 0.50 µM each, consistent with standard chloroplast gene amplifications. Thermal cycling conditions were: initial denaturation at 94 °C for 5 min; 35 cycles of 94 °C for 30 s, 56 °C for 45 s, and 72 °C for 45 s; and a final extension at 72 °C for 5 min. PCRs were performed in technical duplicate for each DNA extract to ensure reproducibility. PCR products were visualised on 1 % agarose gel and high-quality amplicons were submitted for Sanger sequencing (PT Genetika Science, Jakarta). DNA concentration and purity were measured spectrophotometrically using a Thermo Scientific Multiskan Go microplate reader (A_{260} for concentration; $A_{260/280}$ ratio for purity), and DNA extracts with $A_{260/280}$ ratios between 1.8–2.0 were considered acceptable for downstream PCR. Sequencing success was 3/3 (three samples sequenced with high-quality reads) and all consensus sequences matched *P. angulata* accessions in GenBank (100 % identity).

Data Analysis

Morphological and anatomical traits were evaluated descriptively. Forward and reverse sequences of successfully amplified *matK* genes were aligned using BioEdit 7.4 to produce high-quality consensus sequences (Yang et al.

2017). These consensus sequences were then aligned with plant sequences in the GenBank database using the BLAST online tool (https://blast.ncbi.nlm.nih.gov). Phylogenetic relationships were inferred using the Neighbour-Joining (NJ) method implemented in MEGA X, incorporating both sample sequences and reference sequences retrieved from BLAST results (Kumar et al. 2018). The NJ algorithm is a commonly applied approach for constructing phylogenetic trees based on genetic distance (Hong et al. 2021). The *matK* gene sequences from *P. angulata* samples and closely related plant species were used to generate the phylogenetic tree.

RESULTS AND DISCUSSION

Morphological Characters

Leaf and Stem Morphology

Based on the observations, *P. angulata* from the three sampling locations exhibited a herbaceous growth habit, with no variation in overall plant habit. However, leaf characters showed notable variation (Figures 1K and 1L). Variation was observed in leaf shape and margin, whereas leaf apex, surface texture, venation pattern, and colour were consistent across samples. Interestingly, leaf variation was found within the same individual plant. In a single plant, leaves with ovate shapes and either serrated or entire margins could be observed, as well as oblong leaves with either serrated or entire margins. The leaf shapes of *P. angulata* reported by da Silva et al. (2024) also exhibited similar variation, including oblong, ovate, and elliptic shapes. According to García-Verdugo et al. (2019), morphological variation in plants is associated with microevolutionary processes that occur among different plant varieties. The largest leaf blade length was found in the Donggala population, whereas the greatest leaf blade width and petiole length were recorded in the Sigi population (Table 1).

In contrast, stem morphological characters of *P. angulata* were relatively uniform. Observations indicated that the stems were erect with dichotomous branching (Figure 1M). Transverse sections of the stem, observed under a stereomicroscope, revealed that mature stems were round in cross-section (Figure 1J), whereas young stems were angular (Figure 1I). The stems were green in colour and possessed a hollow pith in the centre.

The variation observed in leaf morphology among *P. angulata* individuals may reflect phenotypic plasticity, intra-individual variation possibly due to phenotypic plasticity. Phenotypic plasticity in leaf traits is known to play a crucial role in optimizing photosynthesis, gas exchange, and water use efficiency under fluctuating light and moisture regimes (Arantes et al. 2020). The intra-individual variation is possibly due to phenotypic plasticity (Raymundo et al. 2025). This suggests that both environmental factors such as light intensity, soil moisture, and nutrient availability and intrinsic genetic regulation contribute to the observed morphological diversity.

The uniformity of stem morphology across populations indicates that stem traits are more genetically conserved and less influenced by environmental variation compared to leaf traits. The hollow pith observed in mature stems is a typical characteristic of *P. angulata* and may contribute to structural lightness, allowing the plant to allocate more metabolic resources to reproductive development, particularly flowers and fruits. Taken together, the morphological variation, particularly in leaf characters, highlights the potential for intra-population diversity, which is relevant for conservation studies, breeding programs, and the selection of desirable agronomic traits.

Flower and Fruit Morphology

The floral morphology of *P. angulata* at the three observation sites showed no variation. Flowers are positioned axillarily, exhibiting actinomorphic sym-

Table 1. Leaf blade size and petiole length of *P. angulata* at three observation sites.

Locations	Leaf blade dimensions (cm) (Average ± SD)		Petiole length (cm) (Average ± SD)
	Length	Width	
Parigi Moutong Regency	9.37 ± 1.7	5.04 ± 1.2	3.06 ± 1.0
Sigi Regency	9.26 ± 1.5	5.93 ± 1.0	7.24 ± 1.2
Donggala Regency	9.90 ± 1.1	5.71 ± 0.3	5.70 ± 0.7

metry, and are hermaphroditic. Each flower consists of floral perianth, pistil, and stamens (Figure 1D). The perianth comprises a calyx and corolla. The calyx forms the outer whorl, is green in colour, and consists of five fused sepals. The corolla is located inside the calyx, yellowish-white in colour, and also consists of five fused petals. The stamens are five in number, each comprising an anther and filament, and are free (not fused). The anther is adnate to the filament along its length. The pistil is compound, consisting of a single ovary with three fused carpels, a relatively long and thick style, and a green, disc-shaped stigma.

The floral characters observed in *P. angulata* were similar to those reported for *P. ixocarpa* by Santos et al. (2022), particularly with respect to flower colour and floral whorl number. However, floral diameter and pedicel length were not examined in their study, preventing direct comparison of flower size. The mean floral diameter was nearly identical across the three study locations (Table 2).

The fruit of *P. angulata* is a false fruit (pseudocarp), as the calyx continues to enlarge during fruit development and completely encloses the true fruit, making it invisible from the outside (Figure 1F). The fruit is enclosed by a green calyx with purplish veins (Figure 1G). Mature fruits are spherical and turn yellow upon ripening (Figure 1H). Unlike the flowers, fruit morphology showed variation across the three observation sites. Measured parameters revealed differences in fruit length, fruit diameter, and pedicel length (Table 3). Fruit length is considered one of the key diagnostic characteristics used to distinguish fruit varieties (Zhang et al. 2021). According to Deori et al. (2024), variation in fruit length can be influenced by agronomic practices and environmental conditions.

The absence of variation in floral characters among the three observation sites indicates that the reproductive morphology of *P. angulata* is relatively stable and likely under strong genetic control. This stability is advantageous for pollination success and species recognition, as consistent floral traits ensure effective attraction of pollinators. In contrast, the observed variation in fruit length, diameter, and pedicel length may reflect phenotypic plasticity in response to local environmental conditions or agronomic factors (Medda et al. 2022; Oliva-Ruiz et al. 2023; Bhattarai et al. 2025). Such variation can be used as an important criterion for distinguishing *P. angulata* populations or potential ecotypes, which could be relevant for breeding programs focused on fruit yield or quality.

Anatomical Characters

Leaf Epidermal Structure and Stomatal Characteristics

The epidermis is the outermost tissue layer of the leaf. In *P. angulata*, epidermal cell walls on both adaxial and abaxial surfaces are sinuous but differ in the number of lobes (Figures 2A and 2B). The adaxial surface exhibits fewer lobes (5–7) compared to the abaxial surface (10–12). Similarly, *P. peruviana* also exhibits more lobes on the abaxial surface (12–16) than on the adaxial surface (8–10) (Rodrigues et al. 2021). The shapes of leaf epidermal cell walls are diverse. For instance, members of the genus *Solanum*, which belong to the same family as *P. angulata*, show various wall patterns. Ragab et al. (2022)

Table 2. Flower diameter and pedicel length of *P. angulata* at three observation sites.

Locations	Flower diameter (cm) (Average ± SD)	Pedicel length (cm) (Average ± SD)
Parigi Moutong Regency	2.28 ± 0.1	2.02 ± 0.09
Sigi Regency	2.32 ± 0.2	3.22 ± 0.19
Donggala Regency	2.04 ± 0.1	1.96 ± 0.04

Table 3. Fruit diameter and fruit pedicel length of *P. angulata* at three observation sites.

Locations	Fruit diameter (cm) (Average ± SD)		Fruit pedicel length (cm) (Average ± SD)
	Length	Width	
Parigi Moutong Regency	3.26 ± 0.2	3.24 ± 0.3	3.55 ± 0.3
Sigi Regency	3.22 ± 0.2	1.01 ± 0.2	3.61 ± 0.4
Donggala Regency	3.43 ± 0.1	3.28 ± 0.1	3.56 ± 0.2

reported that leaf epidermal walls in 10 *Solanum* species can be straight, slightly curved, curved, or sinuous, and such variation may occur both among and within species. The abaxial epidermis (77.83 µm) is longer than the adaxial epidermis (73.37 µm). Leaf epidermal traits including the shape of epidermal cell walls, the form and distribution of stomata, and the shape of guard and subsidiary cells are useful diagnostic features for plant identification (Khan et al. 2017).

Stomata are small openings on the leaf surface bordered by a pair of guard cells. In *P. angulata*, stomata consist of a pore flanked by kidney-shaped guard cells and are present on both leaf surfaces. Based on the relationship between stomata and adjacent epidermal cells, *P. angulata* exhibits anomocytic stomata (Figure 2C). These stomata are not surrounded by distinguishable subsidiary cells, as the neighboring cells are indistinguishable from ordinary epidermal cells (Gray et al. 2020). Suwanphakdee et al. (2024) reported that both *P. angulata* and *P. peruviana* growing in Thailand possess anomocytic stomata on both leaf surfaces. Bello et al. (2017) found different stomatal types in 10 *Solanum* species, including anisocytic, anomocytic, paracytic, and diacytic types. Not all *Solanum* species have stomata on both leaf surfaces; for example, *S. paniculatum* and *S. adspersum* are hypostomatic, with stomata restricted to the abaxial surface.

Stomatal size in *P. angulata* did not differ between adaxial and abaxial surfaces. However, Chorchuhirun et al. (2023) reported that *P. angulata* plants growing in Thailand exhibited larger stomata on the adaxial surface (32.67 - 22.07 µm) compared to the abaxial surface (28.42 -18.25 µm). Stomatal density on the abaxial surface was three times higher than on the adaxial surface (Table 4). Stomatal size and density are generally inversely related. Bertolino et al. (2019), who studied plant species with high water-use efficiency, reported that species with larger stomata typically have lower stomatal density and vice versa. Plants with small, densely packed stomata can maximise CO_2 diffusion into the leaf under favourable photosynthetic conditions. The stomatal index of *P. angulata* was nearly twice as high on the abaxial surface. Variation in stomatal shape, size, index, density, and distribution among plant species can affect photosynthetic capacity, and even within the same species, stomatal arrangement may vary depending on leaf morphology and shading conditions (Harrison et al. 2020).

The epidermal and stomatal characteristics observed in *P. angulata* provide valuable insight into its ecological and physiological adaptations (Rashid et al. 2020). The greater number of lobes on the abaxial epidermis and the higher stomatal density on the abaxial surface suggest an adaptation to optimise gas exchange while minimising water loss, a common feature in many mesophytic plants. The presence of anomocytic stomata on both leaf surfaces

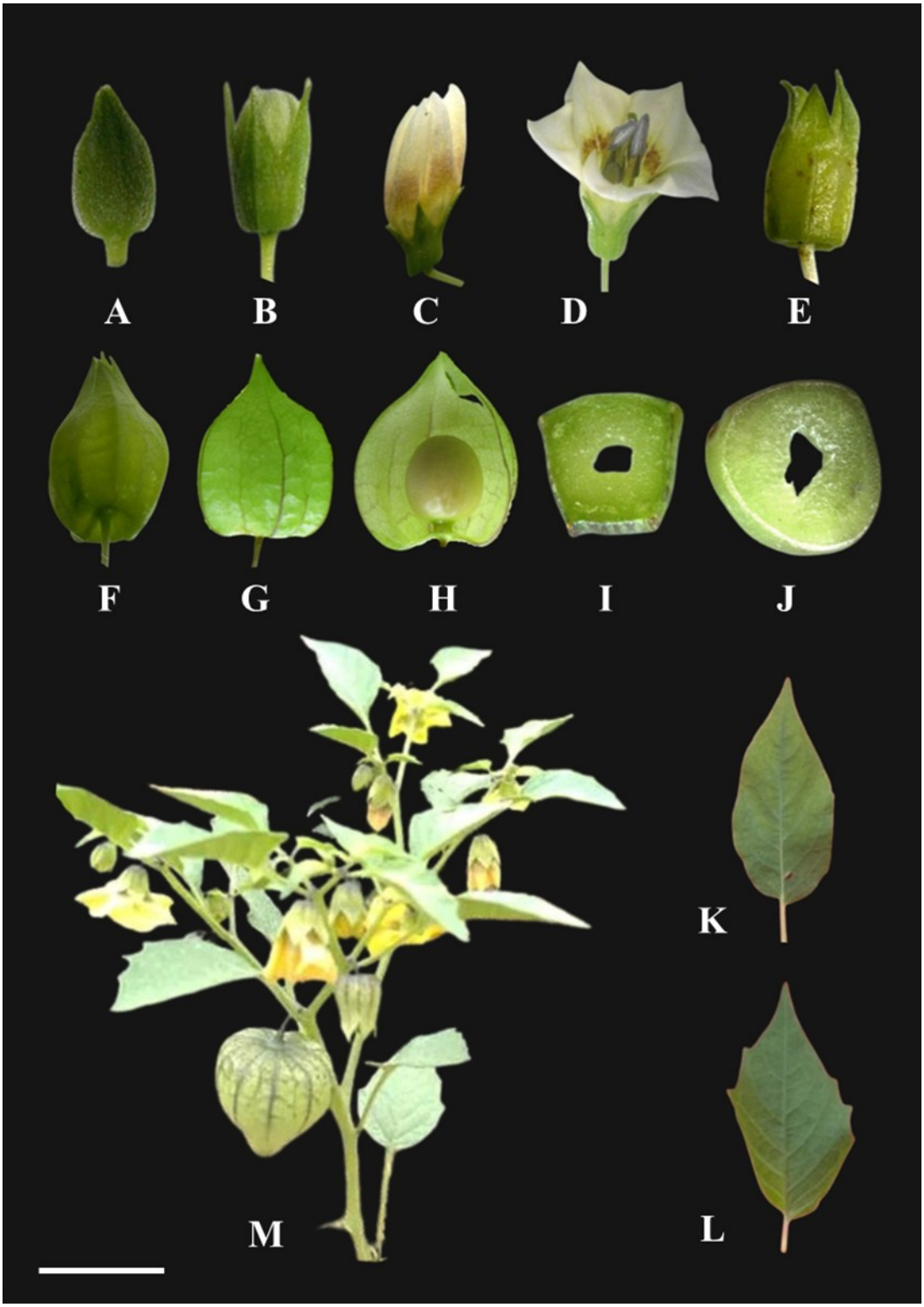

Figure 1. Morphology of *P. angulata*. (A) Early flower bud, (B) Corolla beginning to emerge, (C) Partially opened corolla, (D) Fully opened flower, (E) Calyx enclosing the fruit, (F) Mature fruit, (G) Fruit viewed externally, (H) Fruit viewed internally, (I) Young stem, (J) Mature stem, (K–L) Leaf variation, (M) Whole plant morphology. Scale bar: 1 cm.

indicates amphistomatic leaves, which are typically associated with higher photosynthetic efficiency under optimal light conditions. The inverse relationship between stomatal size and density supports previous findings that plants with smaller, more densely packed stomata are better able to regulate CO_2 diffusion and maintain photosynthetic activity under fluctuating environmental conditions (Driesen et al. 2020). These traits collectively suggest that *P. angulata* possesses a flexible photosynthetic strategy that enables it to thrive in diverse habitats.

Table 4. Stomatal size, density, and index in leaves.

Side	Stomatal size (µm)		Stomatal density (mm^{-2})	Stomatal index
	Length	Width		
Adaxial	31.83 ± 1.8	22.91 ± 1.28	72.67 ± 16.59	17.96 ± 1.5
Abaxial	30.84 ± 1.4	21.28 ± 1.00	209.2 ± 54.00	30.96 ± 2.0

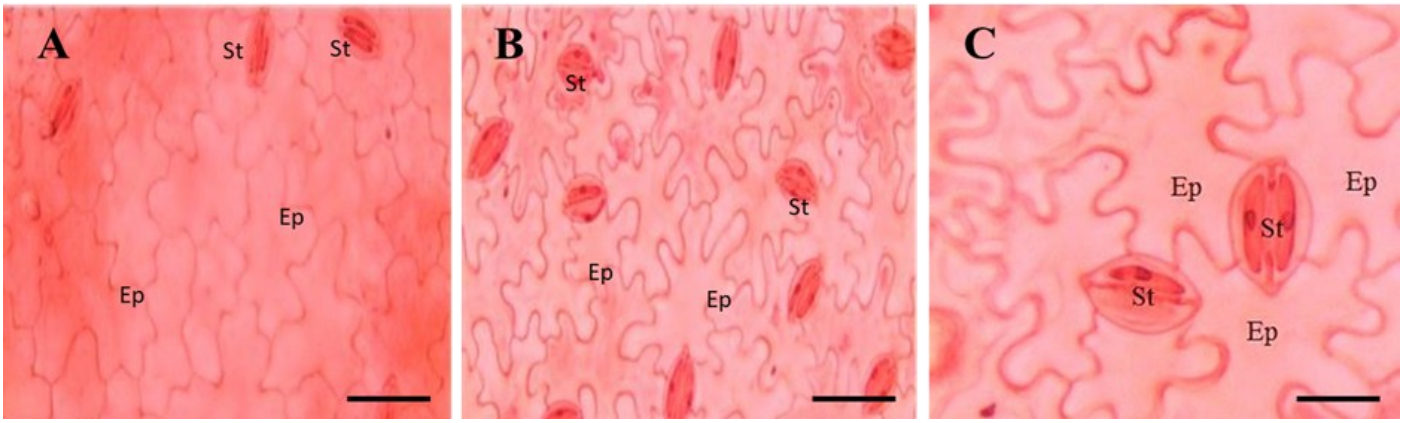

Figure 2. Leaf epidermis of *P. angulata*. (A) Adaxial, (B) Abaxial, (C) Anomocytic stomatal type. Ep: Epidermis; St: Stomata. Scale bar = 100 µm.

Leaf Tissue Structure

The leaf tissue of *P. angulata* consists of the epidermis, palisade mesophyll, spongy mesophyll, and vascular bundles (Figure 3). The epidermis is composed of a single layer of elongated cells. Idioblast cells were also observed between the epidermal layers. The adaxial epidermis is thicker than the abaxial epidermis. A similar pattern was reported in *P. ixocarpa*, where the adaxial epidermis is also thicker than the abaxial epidermis (Silva et al. 2024).

The mesophyll of *P. angulata* is differentiated into palisade and spongy mesophyll tissues. The palisade mesophyll is located above the spongy mesophyll and consists of a single layer of elongated parenchyma cells arranged compactly. According to Stefi et al. (2025), *Origanum vulgare* L. plants growing at high altitudes exhibit high photosynthetic efficiency due to an increased volume of both palisade and spongy mesophyll tissues. The spongy mesophyll of *P. angulata* is located beneath the palisade mesophyll and consists of 4–5 layers of parenchyma cells with varying sizes and large intercellular spaces. Similarly, *P. ixocarpa* has a differentiated mesophyll with a single layer of palisade tissue and approximately five layers of spongy mesophyll (Seleem & Nassar 2021).

Mesophyll tissue plays a critical role in photosynthesis. In *P. angulata*, the palisade-to-leaf thickness ratio was lower (34 %) than the spongy mesophyll-to-leaf thickness ratio (53 %). According to Ni et al. (2022), plants with a high spongy mesophyll-to-leaf thickness ratio are typically found in understory environments as an adaptation to maximise light absorption, since spongy mesophyll tissue is efficient at capturing diffuse light under low-light conditions.

Stem and Root Tissue Structure

A transverse section of the *P. angulata* stem exhibits a circular outline, with a central cavity present in the middle. The anatomical structure of the stem consists of the epidermis, cortex, vascular bundles, and pith (Figure 4). The epidermis is composed of a single layer of elongated cells, with idioblast cells interspersed among them. The cortex, located beneath the epidermis, is composed of collenchyma and parenchyma tissues. The collenchyma is of the lamellar type, characterised by tangential wall thickening, and consists of two layers of elongated cells. The cortical parenchyma is composed of polygonal

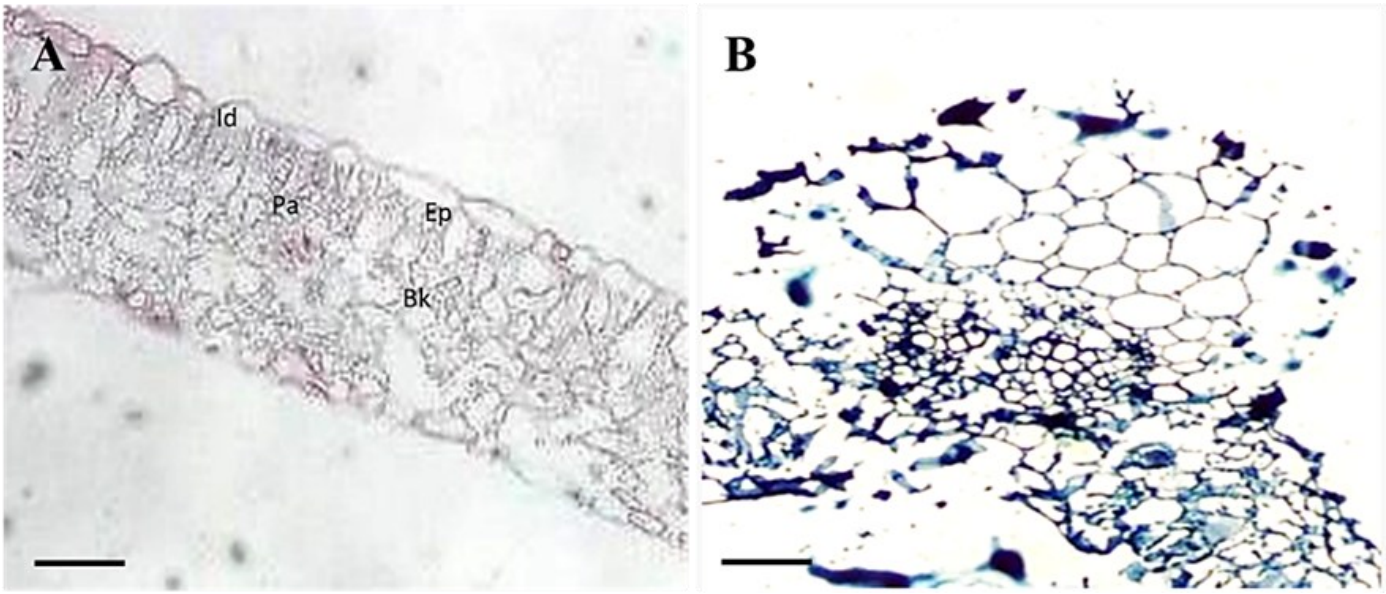

Figure 3. Leaf tissue of *P. angulata*. (A) Transverse section of the leaf, (B) Vascular bundle. Id: Idioblast; Ep: Epidermis; Pa: Palisade; Bk: Spongy parenchyma. Scale bar = 50 µm.

cells.

The vascular bundles of *P. angulata* are of the open collateral type, characterised by the phloem being located external to the xylem, with a cambial layer positioned between them. The cambium consists of 3–4 layers of rectangular cells. This type of vascular bundle has also been reported in other members of the genus, described as a ring-shaped arrangement of open collateral bundles. In addition to the phloem located outside the xylem, *P. angulata* also contains included phloem, which is embedded within the pith parenchyma (Makhmudova et al. 2022; Rajput et al. 2022). The presence of included phloem has also been reported in *Avicennia germinans* (Avicenniaceae), where it occurs within the secondary xylem (Lonard et al. 2017). The pith is composed of hexagonal parenchyma cells that gradually increase in size toward the centre.

The transverse section of the *P. angulata* root reveals a radial arrangement of tissues, consisting of the epidermis, cortex, endodermis, pericycle, and vascular tissues. The epidermis is composed of a single layer of thin-walled cells (Khan et al. 2013). Beneath the epidermis, the cortex consists of several layers of parenchyma cells with large intercellular spaces. The endodermis forms a single, compact layer that regulates the flow of water and nutrients into the vascular cylinder (Barberon 2017). The pericycle lies just inside the endodermis and plays a role in the initiation of lateral roots. The vascular tissues are arranged radially, with xylem and phloem alternating. The central region (stele) is occupied by xylem elements that are relatively well-developed, supporting efficient water and nutrient transport (Madhavan et al. 2025).

DNA Barcoding

PCR Amplification and Sequencing

The *matK* genes were successfully amplified, and the resulting fragments exhibited consistent sizes among individuals. The *matK* amplicons measured approximately 750 bp (Figure 5), which is consistent with the findings of Ilham et al. (2022), who reported a similar fragment size for *matK* in *Achillea millefolium* using the same primers as those employed by Wahyuni et al. (2019).

The amplified *matK* bands exhibited good intensity (Figure 5). As noted by Michel et al. (2016), dense and well-defined DNA bands indicate a high

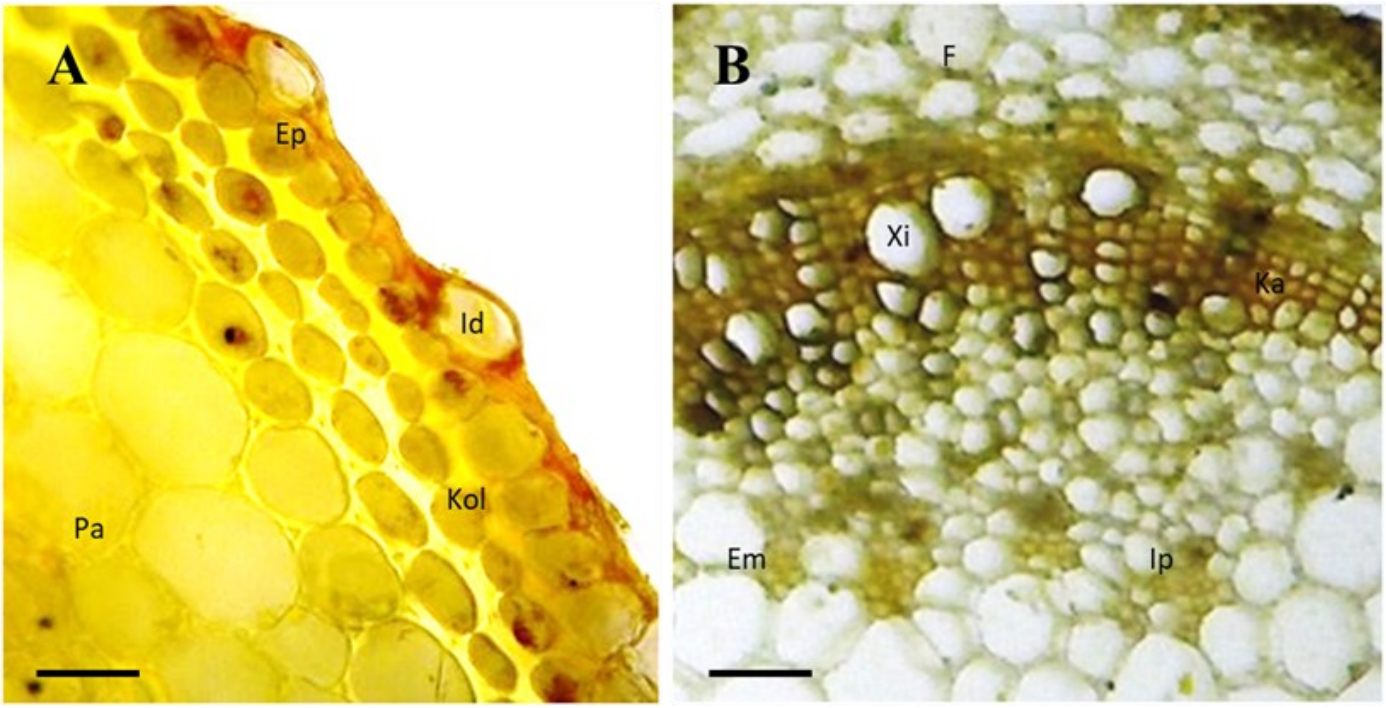

Figure 4. Transverse section of *P. angulata* stem. Id: Idioblast; Ep: Epidermis; Kol: Collenchyma; Pa: Parenchyma; F: Phloem; Ka: Cambium; Xi: Xylem; Ip: Included phloem; Em: Pith. Scale bar = 100 µm.

DNA yield. Band intensity can be influenced by several factors, including primer design, annealing temperature, and DNA polymerase concentration. Primers should be designed to maximise target sequence specificity and maintain an appropriate GC content, both of which are critical for optimising annealing temperature (Kayama et al. 2021). The annealing temperature, in turn, plays a key role in determining PCR product specificity (Kurniawati & Hartati 2018). DNA polymerase serves as the enzyme responsible for synthesising new DNA strands during the PCR process (Garibyan & Avashia 2013).

Sequence alignment using BioEdit 7.4 and MEGA X revealed no gaps in the *matK* gene sequences. Generally, gaps in DNA sequences result from insertion or deletion events (Fan et al. 2007), which are considered major and rapid sources of sequence variation during early eukaryotic evolution (Sanyal et al. 2015). Such mutations may involve a single nucleotide (point mutation) or multiple adjacent nucleotides (segmental mutation) (Flint-Garcia 2013). These genetic changes form the basis of population-level variation and contribute to evolutionary processes through natural selection (Maruzy et al. 2020). Consequently, gaps in DNA barcoding do not indicate failure but can serve as indicators of the potential success of DNA barcoding for the target taxa (Keskin & Atar 2013).

DNA Sequence

The *matK* gene contained 35.5–35.6 % adenine, 18.2 % guanine, 30.2–30.3 % thymine, and 16 % cytosine (Table 5). Overall, adenine and thymine were predominant in the *matK* sequences. This finding is consistent with Smith et al. (2011), who reported that adenine and thymine represent the majority of bases in mitochondrial and plastid genomes. Similarly, Wahyuni et al. (2019) observed that the GC content is lower than the AT content (guanine 42.7 % and cytosine 35.4 %). Based on *matK* sequence data, samples PMR and DR were 702 bp in length, whereas sample SR was 699 bp. The sequences of *P. angulata* obtained in this study showed high similarity to *P. angulata* accessions EF438949.1, EF438950.1, MF159481.1, MF159482.1, and EF438864.1 in the BLAST results, with similarity metrics assessed using % identity, query coverage, and e-values (Table 6).

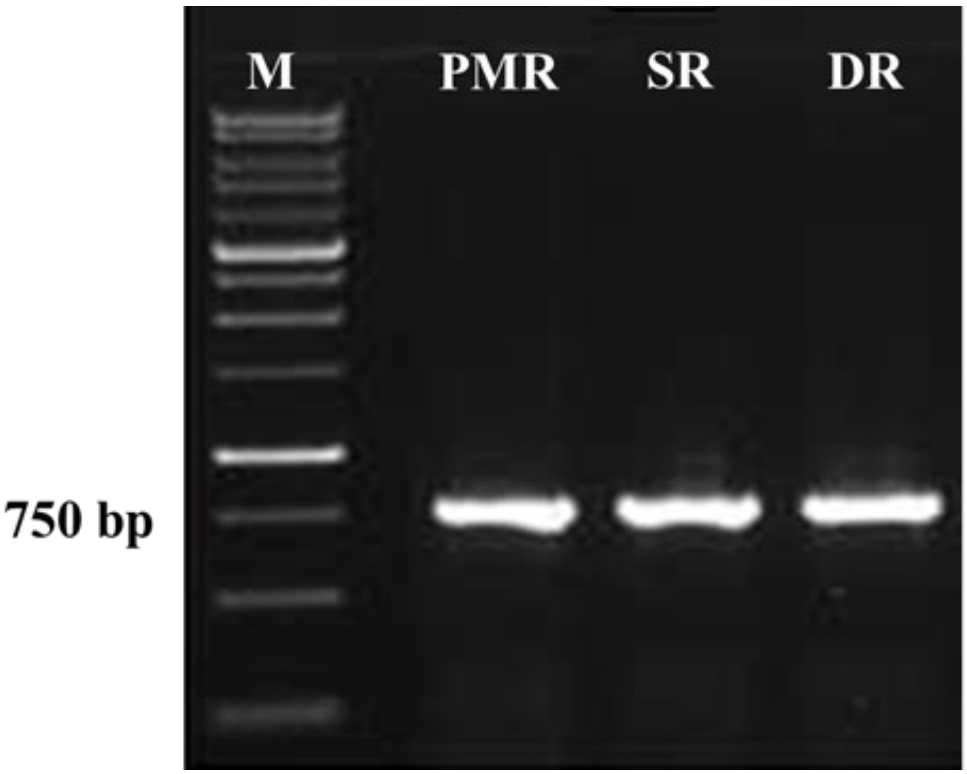

Figure 5. Amplification results of *matK* gene. M = Marker, PMR = Parigi Moutong Regency, SR = Sigi Regency, and DR = Donggala Regency.

The sample sequences and the corresponding GenBank accessions exhibited 100 % identity. When a high degree of identity is observed between an unknown gene sequence and a reference sequence from a recognised species, the two are classified as belonging to the same species. The e-values for these alignments were zero, indicating highly significant matches (Tindi et al. 2017). A BLAST query coverage of 100 % was obtained, which represents the proportion of the sample sequence aligning with the reference sequence (Fathiya et al. 2018). Homology is inferred when the maximum score and total score match, the query coverage approaches 100 %, the e-value is near 0, and the percent identity approaches 100 % (Tindi et al. 2017).

The *matK* gene is widely used as a standard DNA barcode marker due to its classification as chloroplast DNA, which evolves more slowly than nuclear DNA and is thus ideal for inferring phylogenetic relationships among angiosperms (Anzani et al. 2021). Nuclear DNA, in contrast, exhibits greater variability owing to its high recombination rate. Among the four commonly used barcode markers in tropical cloud forest species (*rbcL*, *matK*, *trnH-psbA*, and ITS), *matK* demonstrates relatively high amplification efficiency, sequencing success, and species identification accuracy (Ho et al. 2021). Compared with *rbcL*, *matK* provides greater species-level resolution, as variations in *rbcL* sequences are typically observed at higher taxonomic levels (Anzani et al. 2021).

Phylogenetic Analysis

The phylogenetic tree constructed based on the *matK* gene is presented in Figure 6. The three *P. angulata* samples (PMR.1, SR.1, and DR.1) are positioned within the same cluster, sharing identical branch lengths. The identical branch lengths among taxa indicate no significant variation in nucleotide sequences (Ilham et al. 2022), suggesting that these samples are genetically very closely related. This result is consistent with Anzani et al. (2021), who reported that taxa located on the same branch generally exhibit a very close genetic relationship.

Table 5. Comparison of the number of nitrogenous bases in *P. angulata*.

Samples	Percentage of nitrogen bases	Number of nitrogen bases
PMR	A: 35.6 %, G: 18.2 %, T: 30.2 %, C: 16 %	703
SR	A: 35.5 %, G: 18.2 %, T: 30.3 %, C: 16 %	700
DR	A: 35.6 %, G: 18.2 %, T: 30.2 %, C: 16 %	703

Notes: PMR = Parigi Moutong Regency, SR = Sigi Regency, and DR = Donggala Regency

Table 6. Summary of alignment results of *matK* using BLASTZ.

Scientific Name	Max Score	Total Score	Query Cover	E Value	Per. Ident	Accession
Physalis angulata	1746	1746	100 %	0	100 %	EF438949.1
Physalis angulata	1746	1746	100 %	0	100 %	EF438950.1
Physalis angulata	1746	1746	100 %	0	100 %	MF159481.1
Physalis angulata	1746	1746	100 %	0	100 %	MF159482.1
Physalis angulata	1746	1746	100 %	0	100 %	EF438864.1

Our analysis shows that the three *P. angulata* samples cluster together with other *P. angulata* sequences from GenBank (EF438949.1, EF438950.1, MF159481.1, and MF159482.1). This clade is strongly supported by a high bootstrap value (100 %), indicating robust confidence in the grouping. According to Lemoine et al. (2018), bootstrap values above 70 % are generally considered to represent strong phylogenetic support. Thus, these findings confirm that the three samples analysed are genetically identical to *P. angulata* and are not admixed with other *Physalis* species.

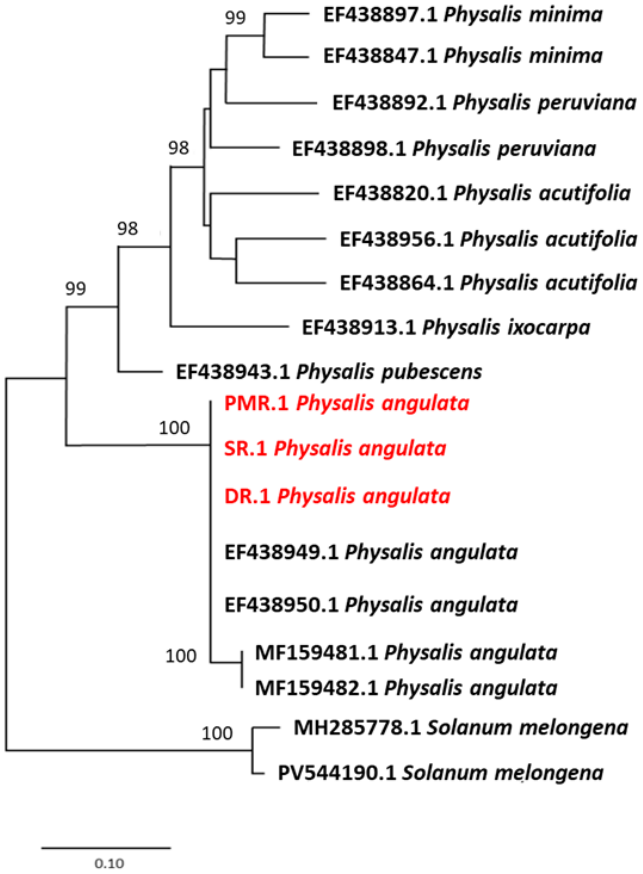

Figure 6. Phylogenetic tree of generated *matK* gene.

In contrast, other *Physalis* species such as *P. pubescens*, *P. ixocarpa*, *P. acutifolia*, *P. peruviana*, and *P. minima* form distinct clades with bootstrap values ranging from 98–99 %, indicating more distant genetic relationships with

P. angulata. This separation is consistent with previously reported morphological characteristics, in which *P. angulata* can be distinguished from other *Physalis* species by its inflated calyx enclosing the fruit, leaf morphology, and flower size (Azeez et al. 2024).

The outgroup used in this analysis was *Solanum melongena* (eggplant), which is positioned on a separate branch and serves as a root to orient the phylogenetic tree. The use of *S. melongena* as an outgroup is appropriate since both *Solanum* and *Physalis* belong to the family Solanaceae but represent different genera, providing sufficient genetic distance to clearly distinguish the *Physalis* clade from its close relatives (Knapp et al. 2013).

Overall, these results confirm the molecular identification of the field specimens as *P. angulata*. This approach is particularly important when morphological characters are difficult to observe due to phenotypic variation or limited flowering/fruiting samples. Accurate species identification supports further studies on the potential utilisation of *P. angulata* as a medicinal plant, which is known to contain bioactive compounds such as withanolides, flavonoids, and alkaloids with anti-inflammatory, anticancer, and immunomodulatory properties (Singirala et al. 2025).

CONCLUSIONS

Based on the results of the study, *P. angulata* exhibits morphological variation primarily in leaf and fruit characters, while flower and stem characteristics remain relatively uniform across locations. Anatomical observations of the epidermis, stomata, mesophyll, stem, and root reveal distinctive structural features that support photosynthetic efficiency, environmental adaptation, and the transport of water and nutrients. DNA barcoding analysis using the *matK* gene successfully identified all samples as *P. angulata* with 100 % similarity to reference sequences, confirming that the observed morphological differences do not indicate separate species but instead represent variation within the same species.

AUTHOR CONTRIBUTIONS

M.T., A.F., and B.A.A. collected and analysed the data and wrote the manuscript. S.M.S. designed the research and supervised all processes.

ACKNOWLEDGEMENTS

We thank staff from the Laboratory of Biology, Faculty of Teacher Training and Education, Tadulako University, Indonesia, for providing facilities during the research. This research was funded by Tadulako University.

CONFLICT OF INTEREST

The authors declare there are no conflicts of interest regarding the research.

REFERENCES

Ahmed, A. et al., 2023. *Gynostemma pentaphyllum* an immortal herb with promising therapeutic potential: A comprehensive review on its phytochemistry and pharmacological perspective. *International Journal of Food Properties*, 26(1), pp.808-832. doi: 10.1080/10942912.2023.2185566.

Ahmed, S. et al., 2022. Pragmatic applications and universality of DNA barcoding for substantial organisms at species level: a review to explore a way forward. *BioMed Research International*, 2022(1), 1846485. doi: 10.1155/2022/1846485.

Antil, S. et al., 2023. DNA barcoding, an effective tool for species identification: a review. *Molecular Biology Reports*, 50(1), pp.761-775. doi: 10.1007/s11033-022-08015-7.

Anzani, A.N. et al., 2021. In silico study of DNA barcoding on soka flower (Ixora). *Prosiding Biologi Achieving The Sustainable Development Goals With Biodiversity I*, 7(1), pp.168-177. doi: 10.24252/psb.v7i1.23693.

Arantes, M.K. et al., 2020. Phenotypic plasticity of leaf anatomical traits helps to explain gas-exchange response to water shortage in grasses of different photosynthetic types. *Theoretical and Experimental Plant Physiology*, 32(4), pp.341-356.

Azeez, S.O. et al., 2024. Anatomical and molecular characterisation in four Nigerian Physalis (Solanaceae) Species. *Nigerian Journal of Botany*, 37 (2), pp.227-250. doi: 10.4314/njbot.v37i2.6.

Barberon, M., 2017. The endodermis as a checkpoint for nutrients. *New phytologist*, 213(4), pp.1604-1610. doi: 10.1111/nph.14140.

Bello, A.O. et al., 2017. Leaf epidermal studies of some Solanum (Solanaceae) species in Nigeria. *Phytologia Balcanica*, 23(1).

Bertolino, L.T. et al., 2019. Impact of stomatal density and morphology on water-use efficiency in a changing world. *Frontiers in Plant Science*, 10, 225. doi: 10.3389/fpls.2019.00225.

Bhattarai, K. et al., 2025. Improvement of crop production in controlled environment agriculture through breeding. *Frontiers in Plant Science*, 15, 1524601. doi: 10.3389/fpls.2024.1524601.

Bolboacă, S.D., 2019. Medical diagnostic tests: a review of test anatomy, phases, and statistical treatment of data. *Computational and Mathematical Methods in Medicine*, 2019(1), 1891569. doi: 10.1155/2019/1891569.

Chorchuhirun, B. et al., 2023. Anatomical Character of *Aglaia cucullata* (Roxb.) Pellegr., a Medicinal Plant Found in Mangrove Forest of Thailand. *Thai Journal of Science and Technology*, 11(4), pp.113-128. doi: 10.14456/tjst.2023.10.

Corvalán, L.C. et al., 2025. Is there a key primer for amplification of core land plant DNA barcode regions (*rbcL* and *matK*)?. *Ecology and Evolution*, 15 (2), e70961. doi: 10.1002/ece3.70961.

da Silva, H.K. et al., 2024. Selection of morphoagronomic descriptors in Physalis angulata L. using multivariate techniques. *Journal of Agricultural Science*, 11(1), pp.289-289. doi: 10.5539/jas.v11n1p289.

Deori, M. et al., 2024. A Comprehensive Review on the Impact of Climate Change on Fruit Yield and Quality in Modern Horticultural Practices. *International Journal of Plant & Soil Science*, 36(1), pp.177-187. doi: 10.9734/ijpss/2024/v36i14348.

Dini, S. et al., 2022. Phytochemical and biological activities of some Iranian medicinal plants. *Pharmaceutical Biology*, 60(1), pp.664-689. doi: 10.1080/13880209.2022.2046112.

Do, H.D.K. et al., 2019. The newly developed single nucleotide polymorphism (SNP) markers forapotent medicinal plant, *Crepidiastrum denticulatum* (Asteraceae), were inferred fromcomplete chloroplast genome data. *Molecular Biology Reports*, 46(3), pp.3287-3297. doi: 10.1007/s11033-019-04789-5.

Driesen, E. et al., 2020. Influence of environmental factors light, CO2, temperature, and relative humidity on stomatal opening and development: A review. *Agronomy*, 10(12), 1975. doi: 10.3390/agronomy10121975.

Ebigwai, J.K. et al., 2020. Application of Maturase K Primer to Determining Nomenclatural identities of Four Morphological Similar Mimosoid Clade Members. *Life Science Journal*, 17(6). doi: 10.7537/marslsj170620.07.

Elhawary, E.A. et al., 2025. Seasonal variation effect on different *Physalis peruviana* L. (Solanaceae) waste extracts and investigation of their efficacy against *Culex pipiens* and *Musca domestica*. *Scientific Reports*, 15(1), 20231. doi: 10.1038/s41598-025-89854-9.

Fan, Y. et al., 2007. Patterns of insertion and deletion in mammalian genomes. *Curr Genomics*, 8(6), pp.370-378. doi: 10.2174/138920207783406479.

Fathiya, N. et al., 2018. Molecular identification of Shorea johorensis in Ketambe Research Station, Gunung Leuser National Park. *Jurnal Natural*, 18(2), pp.56-64. doi: 10.24815/jn.v18i2.10123.

Firdaus, A. et al., 2022. Phenological of cutleaf groundcherry (*Physalis angulata* L.) based on BBCH scale. *Jurnal Agronomi Tanaman Tropika*, 4(2), pp.241-254. doi: 10.36378/juatika.v4i2.2063.

Flint-Garcia, S.A., 2013. Genetics and consequences of crop domestication. *Journal of Agricultural and Food Chemistry*, 61(35), pp.8267-8276. doi: 10.1021/jf305511d.

García-Verdugo, C. et al., 2019. How repeatable is microevolution on islands? Patterns of dispersal and colonization-related plant traits in a phylogeographical context. *Annals of Botany*, 123(3), pp.557-568. doi: 10.1093/aob/mcy191.

Garibyan, L. & Avashia, N., 2013. Polymerase chain reaction. *Journal of Investigative Dermatology*, 133(3), pp.1-4. doi: 10.1038/jid.2013.1.

Gray, A. et al., 2020. Flanking support: how subsidiary cells contribute to stomatal form and function. *Frontiers in Plant Science*, 11, 881. doi: 10.3389/fpls.2020.00881.

Harrison, E.L. et al., 2020. The influence of stomatal morphology and distribution on photosynthetic gas exchange. *The Plant Journal*, 101(4), pp.768-779. doi: 10.1111/tpj.14560.

Hasanuddin & Fitriana., 2014. Relationship fenetik 12 species of Asteraceae family members. *Journal EduBio Tropical*, 2(2), pp.187-250.

Ho, V.T. et al., 2021. Comparison of matK and rbcL DNA barcodes for genetic classification of jewel orchid accessions in Vietnam. *Journal of Genetic Engineering and Biotechnology*, 19(1), 93. doi: 10.1186/s43141-021-00188-1.

Hong, Y. et al., 2021. ENJ algorithm can construct triple phylogenetic trees. *Molecular Therapy Nucleic Acids*, 23, pp.286-293. doi: 10.1016/j.omtn.2020.11.004.

Ilham, M. et al., 2022. Morpho-anatomical characterizationand DNA barcoding of *Achillea millefolium* L. *Biodiversitas*, 23(4), pp.1958-1969. doi: 10.13057/biodiv/d230430.

Kayama, K. et al., 2021. Prediction of PCR amplification from primer and template sequences using recurrent neural network. *Scientific Reports*, 11, 7493. doi: 10.1038/s41598-021-86357-1.

Keskin, E. & Atar, H.H., 2013. DNA barcoding commercially important fish species of Turkey. *Molecular Ecology Resources*, 13(5), pp.788-797. doi: 10.1111/1755-0998.12120.

Khan, R. et al., 2017. Scanning electron and light microscopy of foliar epidermal characters: A tool for plant taxonomists in the identification of grasses. *Microscopy Research and Technique*, 80(10), pp.1123-1140. doi: 10.1002/jemt.22909.

Khan, S.U. et al., 2013. Morpho-anatomical study of selected plants of district bannu, khyber pakhtunkhwa, pakistan. *Pakistan Journal of Weed Science Research*, 19(4).

Knapp, S. et al., 2013. Wild relatives of the eggplant (*Solanum melongena* L.: Solanaceae): new understanding of species names in a complex group. *PLoS One*, 8(2), e57039. doi: 10.1371/journal.pone.0057039.

Kumar, P. et al., 2022. Comparative morpho-anatomical standardization and chemical profiling of root drugs for distinction of fourteen species of family Apocynaceae. *Botanical Studies*, 63(1), 12. doi: 10.1186/s40529-022-00342-z.

Kumar, S. et al., 2018. MEGA X: Molecular evolutionary genetics analysis across computing platforms. *Molecular Biology and Evolution*, 35(6), pp.1547-1549. doi: 10.1093/molbev/msy096.

Kurniawati, S. & Hartati, N.S., 2018. Optimization of the annealing temperature with degenerate primer for amplifiation of arginine decarboxylase (ADC) fragment gene from genomic DNA of Maluku Tenggara local cassava. *Jurnal Ilmu Dasar*, 19(2), pp.135-142. doi: 10.19184/jid.v19i2.6261.

Leelavathy, S. & Sankar, P.D., 2021. Maturase K (*matK*) as a Barcode in Bamboos. *Research Journal of Pharmacy and Technology*, 14(2), pp.955-958. doi: 10.5958/0974-360X.2021.00170.0.

Lemoine, F. et al., 2018. Renewing Felsenstein's phylogenetic bootstrap in the era of big data. *Nature*, 556(7702), pp.452-456.

Lonard, R.I. et al., 2017. The biological flora of coastal dunes and wetlands: *Avicennia germinans* (L.) L. *Journal of Coastal Research*, 33(1), pp.191-207. doi: 10.2112/JCOASTRES-D-16-00013.1.

Madhavan, C. et al., 2025. Anatomical adaptations of mangroves to the intertidal environment and their dynamic responses to various stresses. *Biological Reviews*, 100(3), pp.1019-1046. doi: 10.1111/brv.13172.

Makhmudova, M.M. et al., 2022. Anatomical structure of vegetative organs of medicinal plants *Physalis angulata* L. and their chemical composition. *The American Journal of Agriculture and Biomedical Engineering*, 4 (01), pp.13-21. doi: 10.37547/tajabe/Volume04Issue01-03.

Malik, O.A. et al., 2022. Automated real-time identification of medicinal plants species in natural environment using deep learning models a case study from Borneo Region. *Plants*, 11(15), 1952. doi: 10.3390/plants11151952.

Maruzy, A. et al., 2020. Comparatison study of macroscopic and microscopic characters in three species Phyllanthus L. *Floribunda*, 6(4), pp.154-166. doi: 10.32556/floribunda.v6i4.2020.312.

Medda, S. et al., 2022. Influence of climate change on metabolism and biological characteristics in perennial woody fruit crops in the Mediterranean environment. *Horticulturae*, 8(4), 273. doi: 10.3390/horticulturae8040273.

Michel, C.I. et al., 2016. The nuclear internal transcribed spacer (ITS2) as a practical plant DNA barcode for herbal medicines. *Journal of Applied Research on Medicinal and Aromatic Plants*, 3(3), pp.94-100. doi: 10.1016/j.jarmap.2016.02.002.

Mirzaee, F. et al., 2019. Therapeutic activities and phytochemistry of *Physalis* species based on traditional and modern medicine. *Research Journal of Pharmacognosy*, 6(4), pp.79-96. doi: 10.22127/rjp.2019.93529.

Ni, X. et al., 2022. Variation and determinants of leaf anatomical traits from boreal to tropical forests in eastern China. *Ecological Indicators*, 140, 108992. doi: 10.1016/j.ecolind.2022.108992.

Novitasari, A. et al., 2024. *Physalis angulata* Linn. as a medicinal plant. *Biomedical Reports*, 20(3), pp.1-16. doi: 10.3892/br.2024.1735.

Oliva-Ruiz, M. et al., 2023. Growth, phenotypic plasticity and fruit quality in tomato: a study under high temperature and elevated CO2. *Horticulturae*, 9(12), 1266. doi: 10.1016/j.heliyon.2021.e05988.

Prasetyawan, F. et al., 2024. Morphological analysis of ciplukan plant (*Physalis angulata* L.) pollen for macroscopic identification. *International Journal of Science and Environment (IJSE)*, 4(1), pp.11-17.

Purnobasuki, H. et al., 2017. Morphology of four root types and anatomy of root-root junction in relation gas pathway of *Avicennia marina* (Forsk) Vierh roots. *Vegetos*, 30(2), pp.100-104. doi: 10.5958/2229-4473.2017.00143.4.

Ragab, O.G. et al., 2022. Micromorphological characteristics of leaf epidermis for the identification of certain Solanoideae (Solanaceae). *International Journal of Theoretical and Applied Research*, 1(1), pp.38-48. doi: 10.21608/ijtar.2022.139481.1002

Rajput, K.S. et al., 2022. Inter-and intraxylary phloem in vascular plants: A review of subtypes, occurrences, and development. *Forests*, 13(12), 2174. doi: 10.3390/f13122174.

Rashid, P. et al., 2020. Leaf anatomical adaptation of eighteen mangrove plant species from the Sundarbans in Bangladesh. *Bangladesh Journal of Botany*, 49(4), pp.903-911. doi: 10.3329/bjb.v49i4.52496.

Raymundo, C.E. et al., 2025. Heteroblasty in *Conchocarpus heterophyllus* (A. St.-Hil.) Kallunki & Pirani (Rutaceae): An approach of leaf development from the unifoliolate leaves. *Flora*, 322, 152645. doi: 10.1016/j.flora.2024.152645.

Rivera, D.E. et al., 2019. A screening of plants used in Colombian traditional medicine revealed the anti-inflammatory potential of Physalis angulata calyces. *Saudi Journal of Biological Sciences*, 26(7), pp.1758-1766. doi: 10.1016/j.sjbs.2018.05.030.

Rodrigues, M.H.B.S. et al., 2021. Characterization of physiological maturity of *Physalis peruviana* L. fruits. *Semina: Ciências Agrárias Londrina*, 42(3), pp.929-948. doi: 10.5433/1679-0359.2021v42n3p929

Rouhan, G. & Gaudeul, M., 2020. Plant taxonomy: A historical perspective, current challenges, and perspectives. *Molecular Plant Taxonomy: Methods and Protocols*, pp.1-38. doi: 10.1007/978-1-0716-0997-2_1.

Santos, K.S.D. et al., 2022. Genetic variability of *Physalis ixocarpa* and *P. philadelphica* from physicochemical fruit traits. *Pesquisa Agropecuária Brasileira*, 56, e01534. doi: 10.1590/s1678-3921.pab2021.v56.01534.

Sanyal, G. et al., 2015. Insertion-deletion as informative characters in DNA barcoding. *International Journal of Multimedia and Ubiquitous Engineering*, 10(10), pp.67–74. doi: 10.14257/ijmue.2015.10.10.07.

Schneider, R.F. & Meyer, A., 2017. How plasticity, genetic assimilation and cryptic genetic variation may contribute to adaptive radiations. *Molecular ecology*, 26(1), pp.330-350. doi: 10.1111/mec.13880.

Seleem, E.A. & Nassar, R., 2021. Morphological and anatomical studies on *Physalis peruviana* L. and *Physalis ixocarpa* Brot. Exhornem. *Journal of Plant Production*, 12(11), pp.1179-1183. doi: 10.21608/jpp.2021.100328.1069.

Silva, J.C. et al., 2024. Comparative leaf anatomy of two species of Ipomoea L. (Convolvulaceae): taxonomic importance and adaptations to xeric conditions of the cangas. *PeerJ*, 12, e18599. doi: 10.7717/peerj.18599.

Singirala, S.K. et al., 2025. Extraction of bioactive compounds from *Withania somnifera*: The biological activities and potential application in the food industry: A Review. *International Journal of Food Science*, 2025(1), 9922626. doi: 10.1155/ijfo/9922626.

Smith, D.R. et al., 2011. The GC-rich mitochondrial and plastid genomes of the green alga Coccomyxa give insight into the evolution of organelle DNA nucleotide landscape. *PLoS One*, 6(8), e23624. doi: 10.1371/journal.pone.0023624.

Stefi, A.L. et al., 2025. Oregano young plants cultured at low temperature reveal an enhanced healing effect of their extracts: anatomical, physiological and cytotoxicity approach. *Metabolites*, 15(2), 103. doi: 10.3390/metabo15020103.

Susetyarini, E. et al., 2020. The identification of morphological and anatomical structures of *Pluchea indica*. *Journal of Physics: Conference Series (JPCS)*, 1539, 012001. doi: 10.1088/1742-6596/1539/1/012001.

Suwanphakdee, C. et al., 2024. Characterization of anatomical characters of Peperomia (Piperaceae) from Asia for taxonomy. *Botanical Journal of the Linnean Society*, 205(3), pp.268-291. doi: 10.1093/botlinnean/boad075.

Tindi, M. et al., 2017. The DNA barcode and molecular phylogenetic analysis several bivalve species from North Sulawesi waters based on COI gene. *Jurnal Pesisir dan Laut Tropis*, 1(2), pp.33-38. doi: 10.35800/jplt.5.2.2017.15050.

Wahyuni, D.K. et al., 2019. Morpho-anatomical structure and DNA barcode of *Sonchus arvensis* L. *Biodiversitas Journal of Biological Diversity*, 20(8), pp.2417-2426. doi: 10.13057/biodiv/d200841.

Wahyuni, D.K. et al., 2022. Morpho-anatomical characterization and DNA barcoding analysis of *Pluchea indica* (L.) Less. *Biodiversitas Journal of Biological Diversity*, 23(8). doi: 0.13057/biodiv/d230851.

Wahyuni, D.K. et al., 2024. Morpho-anatomical characterization and DNA barcoding of *Artemesia vulgaris* L. *Brazilian Journal of Biology*, 84, e278393. doi: 10.1590/1519-6984.278393.

Wang, M. et al., 2024. From species to varieties: How modern sequencing technologies are shaping Medicinal Plant Identification. *Genes*, 16(1), 16. doi: 10.3390/genes16010016.

Yang, J. et al., 2017. Development of chloroplast and nuclear DNA markers for Chinese oaks (Quercus Subgenus Quercus) and assessment of their utility as DNA Barcodes. *Frontiers in Plant Science*, 8, 816. doi: 10.3389/fpls.2017.00816.

Yue, J. et al., 2021. Application of identification and evaluation techniques for ethnobotanical medicinal plant of genus Panax: A review. *Critical Reviews in Analytical Chemistry*, 51(4), pp.373-398. doi: 10.1080/10408347.2020.1736506.

Zhang, X. et al., 2021. Quantitative extraction and analysis of pear fruit spot phenotypes based on image recognition. *Computers and Electronics in Agriculture*, 190, 106474. doi: 10.1016/j.compag.2021.106474.